Mining of Mineral Deposits
Volume 16 (2022), Issue 3, 38-47

MMD JOURNAL / MINING.IN.UA

https://doi.org/10.33271/mining16.03.038

Multivariate statistical-based approach to the physical-chemical behavior of shallow groundwater in a semiarid dry climate: The case study of the Gadaïne-Ain Yaghout plain NE Algeria

Imane Dib[1]✉, Abdelhamid Khedidja[2]✉, Wahid Chattah[3]✉, Riheb Hadji[1*]✉

[1] *Setif University, Setif, Algeria*
[2] *University of Batna, Batna, Algeria*
[3] *University of Constantine, Constantine, Algeria*

**Corresponding author: e-mail hadjirihab@yahoo.fr*

Abstract

Purpose. Several natural and anthropogenic factors control the hydro-geochemical behavior of groundwater. These factors influence on the quality, even the suitability of this resource for drinking. The main purpose of our study is the application of multivariate statistical methods to compile the mechanisms of mineralization acquisition in confined aquifers.

Methods. The adopted method measures the chemical evolution of Ca^{+2}, Mg^{+2}, Na^{+}, K^{+}, HCO^{-3}, Cl^{-}, $SO4^{-2}$, NO^{-3}, NO^{-2}, NH^{+4}, and PO_4^{-3} using an atomic-absorption spectrometer. The content of nitrogen and dissolved oxygen is measured using a spectrophotometer. Temperature (T°), electrical conductivity (EC), pH and dissolved oxygen are determined using a multi-parameter system.

Findings. The main results show that 28 water samples from the Mio-Plio-Quaternary aquifer of the Gadaïne-Ain Yaghout plain have chemical facies of chloride, sulfate-calcium and chloride-magnesium types.

Originality. The originality of the study is in the demonstration that water acquires its carbonate mineralization at the supply limits. Whereas it acquires its chloride, sodium and sulfate mineralization in contact with terrigenous saliferous formations, as well as in its interaction with the salt chotts formations. The results show a significant variation in the concentrations of chemical elements, in some cases exceeding drinkability standards. Mineralization is mainly caused by the dissolution of evaporitic minerals such as gypsum, halite and epsomite.

Practical implications. The practical implications of this study could be resumed in terms of the convenience of multivariate statistical evaluation of complex physical-chemical databases in identifying pollution sources and understanding temporal variations for effective groundwater quality management in semiarid regions.

Keywords: *semiarid, shallow aquifer, physical-chemical, multivariate, pollution*

1. Introduction

The chemical composition of groundwater can be influenced by several natural and anthropogenic factors [1]-[7]. Natural processes that affect water quality include dissolution, precipitation rate and chemical saturation of water, while human activities include over-pumping of the aquifer, domestic and industrial discharges, as well as agricultural practices [8]-[12]. Therefore, the sustainable management of potable-quality water requires proper control of the geochemical behavior of the aquifer [13]-[20]. The deterioration of the physical-chemical quality of the waters in the endorheic basins of NE Algeria is caused by the dissolution of carbonate rocks, chott salinization, and the improper use of nitrogen fertilizers in agriculture [21]-[24].

Standard multivariate statistical analysis methods such as Principal Component Analysis (PCA) and/or Factor Analysis (FA) have been extensively applied to analyze groundwater quality data in different aquifers around the world [25], [26]. These approaches are able to oversimplify groundwater-quality data by reducing the amount of parameters to a small number of factors, while extracting significant groundwater information. This makes it possible to identify predictive variables for the geochemical behavior of water resources [27]-[29].

The pollution of the Gadaïne-Ain Yaghout aquifer is influenced by the dissolution of Triassic and carbonate deposits, as well as domestic discharges and the improper use of chemical fertilizers. The repeated use of these waters poses a major public health problem. To address this issue, our study monitored the current state of water quality and the spatial distribution of pollutants. For this task, we conducted a sampling campaign to identify the physical-chemical composition of waters [30]. Our study aims to address the lack of knowledge about the hydro-chemical evolution control of waters in semiarid regions. The main attention is paid to the behavior of polluting elements in the groundwater of the Gadaïne-Ain Yaghout plain. Firstly, we investigated the variation of physical elements in shallow aquifers. Then,

Received: 20 May 2022. Accepted: 14 August 2022. Available online: 30 September 2022

Mining of Mineral Deposits. ISSN 2415-3443 (Online) | ISSN 2415-3435 (Print)

using PCA and FA, we characterized the physical-chemical properties of water to demonstrate the relationship between the elements and factors controlling the distribution of Ca^{+2}, Mg^{+2}, Na^{+}, K^{+}, HCO_3^{-}, Cl^{-}, SO_4^{-2}, NO_3^{-}, NO_2^{-}, NH_4^{+} and PO_4^{-3} elements.

2. General setting

The Gadaïne-Ain Yaghout plain is located in the north-east of Algeria between the latitudes 35°40′36.10″ to 35°54′8.88″ and longitudes 6°13′22.79″ to 6°30′36.94″. This plain belongs to the NW fringe of the high plains in the southern Constantine, between the Neritic and the Atlas zones (Fig. 1). Mio-Plio-Quaternary (MPQ) formations filled the plain on a Jurassic-Cretaceous carbonate substrate outcropping at the edge of the basin [31], [32]. This plain is mainly agro-pastoral with an intensive cereal crop cultivation on an area of 10 731 ha. The Gadaïne-Ain Yaghout region is characterized by a semiarid climate with an average annual rainfall of 338 mm and an average temperature of 15°C. The runoff, estimated by the empirical formula of Tixeront and Berkaloff, benefits from only 5.3% of precipitation, while infiltration is only 1.06% [33]. There are two levels of aquifers; one shallowly is characterized by heterogeneous MPQ formations of lacustrine limestone, alluvium and clays facies. The groundwater table of this aquifer can either be basic in the chott of Gadaïne, or free or semi-free in its vicinity. This aquifer is recharged by carbonate reliefs at the boundaries, as well as by effective precipitation [34]. Deep carbonate formations from the Jurassic and Cretaceous periods constitute the second aquifer. Its recharge occurs due to the foothills of massifs, as well as the runoff of surface water in the absence of waterproof screen in place and at fracture level [35].

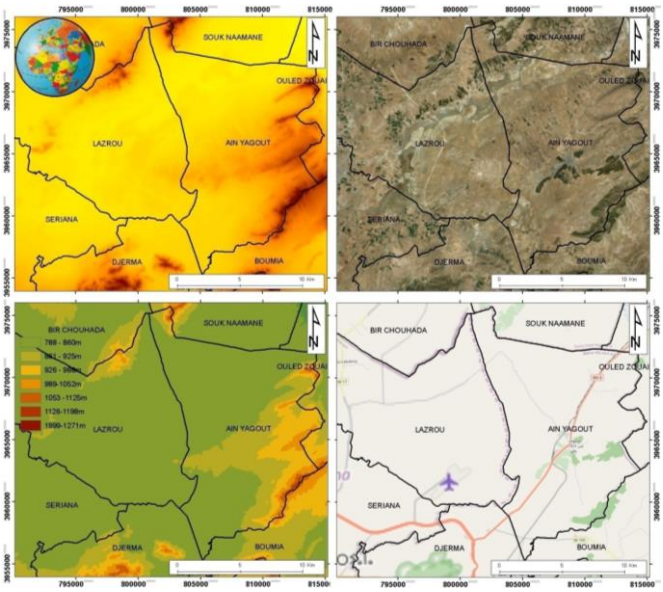

Figure 1. Geographic location of the study area

The piezometric maps of the study area show that the waters flow converges towards a drainage zone located in the foothills of the Tizourit and Guedmane massifs [36], [37]. In contrast to the bottom of the plain occupied by the Gadaïne and Tenet Saida chotts, where the water is drained by the Tinsilt chott, the piezometric depression mainly reflects the excessive exploitation of the water table by a large number of wells and boreholes, intensified by the acute drought caused by climate change [38].

3. Methods

We conducted a sampling campaign at the end of the flood period (June 2018) to analyze physical-chemical properties of groundwater in the Gadaïne-Ain Yaghout region. Twenty-eight (28) water samples have been taken at various locations throughout the study region, including water points (boreholes) located throughout the plain, to determine water quality (Fig. 2).

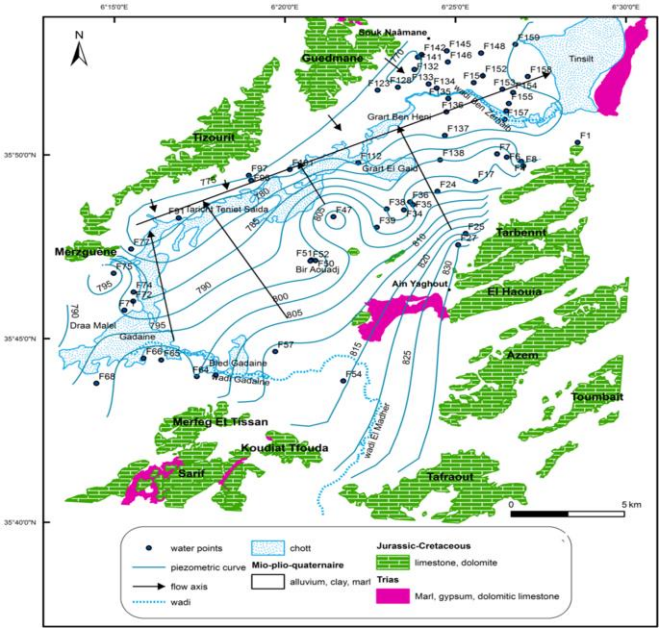

Figure 2. Natural conditions of the Gadaïne-Ain Yaghout region

A graphic and cartographic representation of the physical-chemical characteristics is used to conduct this analysis [39]. Chemical analyzes were performed at the Horizon Laboratory in Annaba (H.L.A.). The chemical elements Ca^{+2}, Mg^{+2}, Na^{+}, K^{+}, HCO_3^{-}, Cl^{-},SO_4^{-2},NO_3^{-}, NO_2^{-}, $NH_4^{+}$and PO_4^{-3} were measured using an atomic absorption spectrometer for cations and titration assay for chlorides and alkalinity [40].

Spectrophotometry was used to measure the elements of nitrogen and dissolved oxygen. Sodium paranitosalicylate of yellow color (415 nm) is formed by nitrates in the presence of silicates. A portable multi-parameter system type WTW LF197 was used to measure temperature (T°), electrical conductivity (E.C.), pH, and dissolved oxygen on the ground [41]. In order to know the reliability of our chemical results, the ionic balance calculated for all analyzed water samples is estimated at about 5% for all samples. All mapping of the various studied parameters is performed using the GIS technique [42]-[46]. The statistical processing was carried out using the Statistics and Phreeqc-2 (V 2.10) program [47], [48].

4. Results and discussion

We have presented and interpreted the observed qualitative physical-chemical trends to make the results easier to use. Therefore, we provide interpretation results to determine the natural or anthropogenic origin of the elements found (Table 1). Descriptive statistic of physical-chemical analyzes of the Gadaïne – Ain Yaghout plain groundwater (Table 2) is intended to summarize the observations on the state of its qua-lity. It has been revealed that for the average values, there is a predominance of the HCO^{3-}, Cl^{-}, $SO4^{-2}$, and Ca^{+2} elements over the other parameters.

Table 1. Descriptive statistics of the physical-chemical groundwater parameters in the study area

Parameters	Standards		Maxi	Min	Average	SD dev
	AWS	WHO(2017)				
CE (µS/cm)	2800	–	13650	1320	4950	2.78
pH	6.5 à 9	6.5 à 8.5	8.3	7.75	7.99	0.12
T (ºC)	25	–	24	16	19.18	1.93
O_2 (mg/l)	–	–	13.2	6.2	10.14	1.79
Ca^{2+} (mg/l)	200	100	3145	428.8	1027.25	553.78
Mg^{2+} (mg/l)	–	< 100	1144	139	371.34	203.86
Na^{+} (mg/l)	200	200	1420	58	414.86	328.53
K^{+} (mg/l)	12	250	20	1	9.26	5.35
Cl^{-} (mg/l)	500	200 à 300	5538	397.6	1922.07	1037.55
SO_4^{2-}(mg/l)	400	< 250	3000	290	1179.64	716.84
HCO_3^{-}(mg/l)	–	–	6439.5	878.2	2103.44	1133.90

Nb: the Algerian Water Standards (AWS) were set by decree No. 14-96 of March 4, 2014, defining the quality of water for human consumption

In this case, the average values of electrical conductivity and dissolved oxygen is also higher or lower. In addition, each physical parameter appears to have some homogeneity; however, the chemical parameters exhibit significant heterogeneity.

4.1. Spatial variation of the physical-chemical parameters

4.1.1. Electrical conductivity (EC)

The spatial EC distribution (Fig. 3) shows two distinct zones: the first with EC from 1000 to 5000 µS/cm, observed at the East and southwest of the plain, and near Jebel Guedmane. In the vicinity of the Ain Yaghout Mountains, water points have values of < 2800µS/cm. These values are influenced by the direct feeding from these landforms. The second value EC > 5000 µS/cm is observed in the chotts area. At the Tinsilt chott boundary, the maximum value reached 13650 µS/cm. This contrast of variation shows an increase in mineralization in the groundwater flow direction.

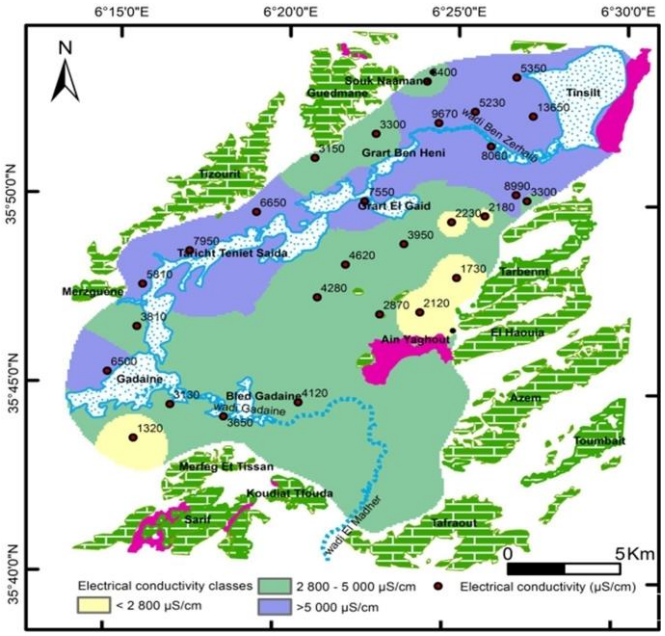

Figure 3. The Electrical conductivity map of the study area

The excessive mineralization of these waters can be explained by the longer migration time in the aquifer, which allows a greater quantity of minerals to pass into solution from the crossed formations, in particular, evaporitic and Triassic soils. In addition, the increase in conductivity is related to the evaporation of near-surface water, agricultural activities and the discharge of urban wastewater containing chlorides.

4.1.2. Evaporitic elements

In all water samples, the calcium level exceeds the Algerian standard (200 mg/l). The highest values were recorded near the Tizourit carbonate massif, to the northeast of the plain and at the F69 drilling site; while, at the water wells N°F42 and F27 in the feeding zone, a range of 428.8 mg/l was measured. However, moderately high concentrations (about 1000 mg/l) are found in the F65 well, located near wadi El Madher, where the treated wastewater from the city of Batna and the untreated wastewater from the village of Ain Yaghout are discharged. The standard deviation value is 553.78, which reflects a large variation in the content, because the Ca^{2+} ion is of both natural and anthropogenic origin.

The Mg^{2+} content ranges between 139 and 1144 mg/l. This increase in concentration is conditioned by the numerous reactions of cation exchange, adsorption and desorption on clay minerals, which influence on the magnesium dissolution of in the underground environment from clays and marls present in the plain, as well as dolomites constituting the reliefs. The spatial distribution of the Mg^{2+} ion is identical to that of calcium. The sodium content is between 58 and 1420 mg/l, of which most of these concentrations are outside the Algerian standard of drinkability (200 mg/l). Excessive Na^{+} values are observed near the Taricht, Teniet Saida, Grart El Gaïd chotts and around the Tinsilt chott, where evaporitic formations are very abundant. So these values are completely consistent with geological characteristics.

The K^{+} element concentration ranges from 1 to 20 mg/l, which is caused by the alteration of potassium clays and chott evaporites. They are located at the F134 and F158 wells, where intense agricultural activity is carried out with the use of chemical fertilizers rich in potassium, such as: "Mairol vert 14/12/14" and "Verdicrop 12/12/36".

Except for the F42 borehole (397.6 mg/l), chloride levels recorded in groundwater are generally higher than Algerian drinking water standards (500 mg/l) with levels ranging from 781 to 5538 mg/l. These values are dominant compared to other elements. This indicates the existence of a very important salt contribution of clays, Triassic marls, and evaporitic formations. The most significant concentrations are found in the vicinity of the chotts. The reason for the increased concentrations in the analyzed water may be anthropogenic inputs related to domestic water discharges, the use of chemical fertilizers containing potassium chloride, and, as a result, irrigation water discharges.

The values of the sulfate content in the analyzed waters are within the range of the Algerian standard (400 mg/l).

They are observed at the level of boreholes F27 (east of the plain) and F67 (southwest of the plain). Whereas the highest concentrations (> 2500 mg/l) are measured at F97, F112, and F158 water points. These contents are concentrated at the level of the chotts after the dissolution of the Triassic gypsum and evaporites, enrichment of which in this element on the plain occurs in the direction of the groundwater flow. However, the anthropogenic origin of sulfates is not excluded at the points with the highest concentrations due to the use of sulfate-ammonium type fertilizers.

In addition, the sulfate content is very dependent on the redox potential of the medium. The analyzed waters are rich in oxygen (typical for a shallow aquifer), which contributes to the oxidation of sulfide minerals and the formation of $SO4^{-2}$ ions in solution.

4.1.3. Carbonate elements

Analyzes indicate a bicarbonates content between 878.2 and 6439.5 mg/l and a high standard deviation of 1133.90. Enrichment in HCO^{3-} is observed in all analyzed waters, especially in the southern foothill of the "Tizourit" carbonate massif and closer to the northeast of the plain. This enrichment is certainly caused by the water-rock interactions (limestone and dolomites of the Jurassic-Cretaceous formations) with HCO^{3-} release.

4.1.4. Nitrogenous elements and heavy metals

The descriptive statistic of the results of analyzes of nitrogenous, phosphorus and metallic elements in trace amounts (heavy metals) of the Gadaïne – Ain Yaghout groundwater (Table 2) shows that each element presents certain homogeneity.

Table 2. Nitrogenous, phosphorus and metallic elements in trace amounts in groundwater

Standard elements	Standards		Max (mg/l)	Min (mg/l)	Average (mg/l)	STD Dev
	AWS	WHO (2017)				
NO_3^-	50	50	66	24	30.5	7.85
NO_2^-	0.2	3	0.6	0.09	0.19	0.09
NH_4^+	0.5	–	0.93	0.13	0.3	0.17
PO_4^{3-}	5	–	12.4	7.2	8.68	1.09
Zn^{2+}	5	≤ 4	2.3	0.02	0.36	0.45
Cu^{2+}	2	2	0.44	0.003	0.08	0.11
Fe^{2+}	0.3	≤ 0.3	0.35	0.014	0.05	0.07
Cd^{2+}	0.003	0.003	0.31	0.010	0.08	0.08
Sr^{2+}	–	–	0.131	0.014	0.04	0.03

4.1.5. Nitrates (NO_3^-), nitrites (NO_2^-) and phosphate (PO_4^{-3})

In the analyzed groundwater, nitrate content has been revealed in the range of 24-38 mg/l. However, there is only one point (F112) where the value exceeds 50 mg/l, with the maximum value of 66 mg/l. This content may reflect an anthropogenic input, due to which nitrates can enter groundwater; by leaching after excessive application of inorganic nitrogen fertilizers and manure from the wastewater effluents from the municipal facilities of Ain Yaghout and discharged into wadi El Madher.

Nitrites values in 28 samples range from 0.09 to 0.6 mg/l and exceed the ADE standard (0.2 mg/l) in 8 samples. These points are located in the center of the plain, where reducing conditions prevail at this time of the year; the soils have not yet been plowed and therefore will not be well aerated. Ammonium was found in all water points. The concentrations observed during this campaign are generally between 0.13 and 0.93 mg/l with a relatively low standard deviation (0.17). These concentrations exceed the standard (0.5 mg/l) in three samples: F97, F112 and F158. The highest ammonium content (more than 0.5 mg/l) is measured in the least oxygen-rich water (the concentration of dissolved oxygen is 8.8, 6.9 and 9.7 mg/l, successively).

For phosphates, groundwater analyzes have revealed levels much higher than the ADE standard (5 mg/l) and then ranging from 7.2 to 12.4 mg/l. Of the 28 points, three have concentrations exceeding 10 mg/l, namely F69 and F112 (located in succession next to the chott de Gadaïne and Grart El Gaïd), as well as F63 (next to wadi El Madher).

4.1.6. Heavy metals

Trace amounts of zinc were identified in all analyzed samples. The levels ranging from 0.02 to 2.3 mg/l are lower than the guide value proposed by ADE (5 mg/l), given that the maximum was recorded at point F112 (Fig. 4). Sphalerite leaching from the liasic dolomites of Jebel El Haouia (in Ferkous H., 2007) may be a natural source of zinc in these waters. The agricultural origin (manure, slurry and fertilizers) also determines the occurrence of Zn^{+2} in the analyzed waters. Copper was identified in all sampled points, with a maximum of 0.44 mg/ballast recorded in a sample (F112) located in clays with the binding capacity of this element. Its concentrations range between 0.003 (F69) and 0.44 (F112) mg/l and remain well below the Algerian and WHO standard (2 mg/l). Excluding the value of 0.35 mg/l (F112) of iron (Fe^{+2}), which exceeds the content set by ADE, observed concentrations are generally between 0.014 and 0.19 mg/l and remain below the standard (0.3 mg/l). For cadmium, only three samples F27, F42 and F113 with concentrations of 0.002, 0.001 and 0.002 mg/l, respectively, are below the threshold set by WHO and ADE. The increased levels ranging from 0.21 to 0.31 mg/l are recorded in the northeast of the plain. Strontium was found in all analyzed water samples with content from 0.014 to 0.131 mg/l. These values remain below 7 mg/l (this is a maximum acceptable concentration (MAC), proposed by the Federal-Provincial-Territorial Committee on Drinking Water (CEP) of Canada).

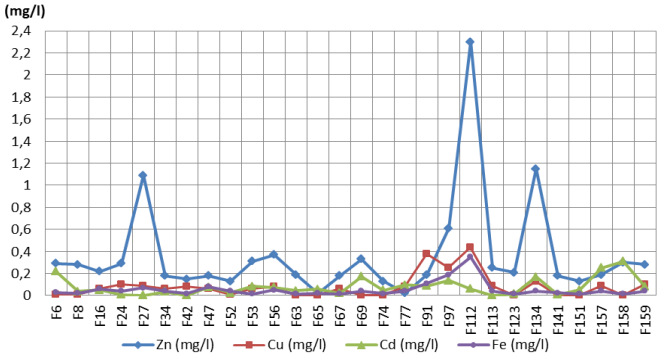

Figure 4. Variation of the heavy metal content in the groundwater of the study area

Chemically, strontium is similar to calcium, which it replaces in carbonate rocks. Sedimentary environment seems to be the most favorable contexts for the occurrence of strontium in water, in particular, evaporite levels rich in celestine ($SrSO_4$), a mineral often associated with Triassic gypsum ($CaSO_4\,2H_2O$). Consequently, high strontium concentrations

are localized at the level of chotts, which enter from the leaching of limestone from marginal reliefs under the influence of the direction of the underground flow.

4.2. Water-chemical facies

The presentation of the chemical analysis results on the Piper diagram made it possible to reveal that 60% of the waters have a chloride and sulfate-calcium facies, and 40% of the waters have a sulfate-magnesium facies (Fig. 5).

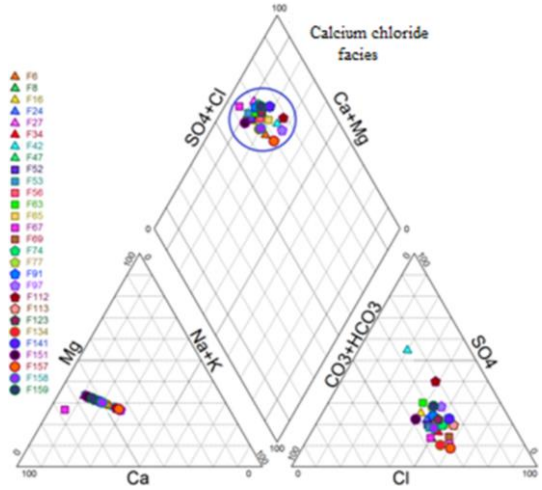

Figure 5. Piper diagram of the analyzed samples

Both facies indicate that natural mineralization is probably the result of the influence of aquifer formations (such as clays, carbonates, marls and Triassic gypsum) to acquire groundwater ionic mineralization, as well as an evaporative process that concentrates evaporite-forming elements at the chott level. The presence of fractured and karstified limestone formations at the boundaries indicates infiltration of precipitation waters, where they acquire their initial bicarbonate-calcium mineralization, which explains the low salinity of waters at these boundaries. These waters are more mineralized with chlorides, sodium and sulfates on contact with terrigenous saliferous formations due to the dissolution of salt minerals, Base Exchange with clays and concentration of water in chemical elements according to the direction of underground flow. However, the anthropogenic origin of chlorides, sulfates and calcium is not excluded. Elevated concentrations in the analyzed water are caused by domestic water discharges, the use of fertilizers, and irrigation water discharges.

The analyzed samples presented in the Chadha diagram (Fig. 6) show water of the "chloride-calcium-magnesium" type for all waters of the plain, where alkaline earths (Ca^{+2} + Mg^{+2}) prevail over alkalis (Na^{+} + K^{+}), and the couple (Cl^{-} + SO_4^{-2}) prevail over bicarbonates (HCO_3^{-}). Waters of this type acquire their mineralization in the process of reverse ion exchange; therefore, when irrigated, they do not deposit residual sodium carbonate. The "chloride-calcium-magnesium" indicates a mixture of water from a shallow aquifer with water from a deep aquifer.

4.2.1. Water-rock interaction

Water-rock interactions and fluid circulations are recognized as the main agents of matter mobilization and transportation. Thus, the chemical composition of groundwater reflects the mineralogical composition of host rocks and can be used to localize recharge areas, the origin of groundwater (meteoric, marine, fossil, magmatic and metamorphic) and different chemical compounds (carbonate, sulfate, nitrate and ammonium).

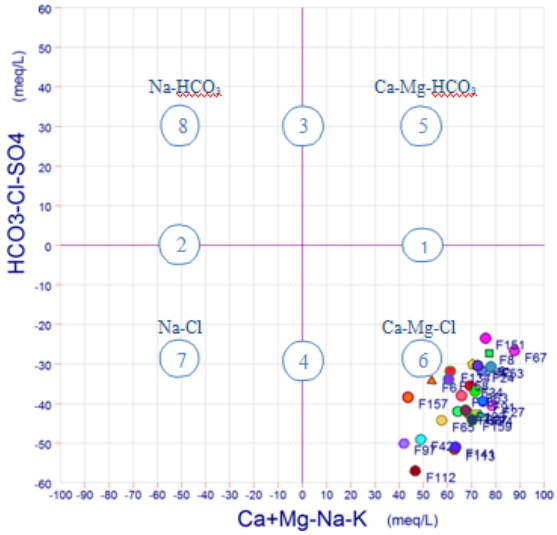

Figure 6. Chadha diagram of the study area

Water chemistry can also provide information about water-rock interaction processes [49], [50]. The Gibbs graph showing variations in Na/(Na + Ca) and Cl/(Cl + HCO_3) ratios as a function of Total Dissolved Solids "TDS" (Fig. 7) indicates that 82% of the samples are influenced simultaneously by the process of evaporation and precipitation, while 18% are controlled only by the action of evaporation.

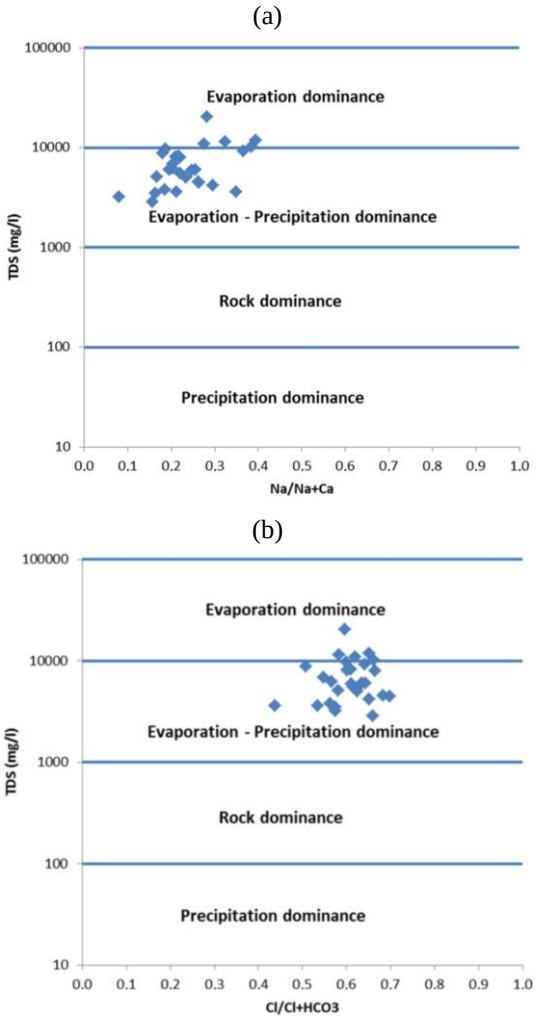

Figure 7. Binary Gibbs diagrams explaining the origin of elements and the dominant chemical processes: (a) for cations; (b) for anion

Surface water and moisture present in the unsaturated zone is concentrated by evaporation, resulting in the precipitation of evaporites that are eventually leached into the saturated zone. Given the intensification of irrigation activities associated with the shallow water depth in agricultural regions, evaporation has become the major factor in the concentration of ions, which causes an increase in salinity and TDS (TDS max = 20483 mg/l).

4.3. Statistical analysis

4.3.1. Multivariate statistical analysis

Principal Component Analysis (PCA) is a multidimensional exploratory statistical tool. It is one of the most widely used multivariate data analysis methods. It allows you to explore multidimensional datasets made up of quantitative variables. The data were processed using a reduced centered PCA on a rectangular array of 20 variables (EC, T, pH, O_2, Ca^{+2}, Mg^{+2}, Na^{+}, K^{+}, Cl^{-}, SO_4^{-2}, HCO_3^{-}, NO_3^{-}, NO_2^{-}, NH_4^{+}, PO_4^{-3}, Fe^{+2}, Zn^{+2}, Cu^{+2}, Cd^{+2} and Sr^{+2} and 28 individual samples, using XLSTAT software).

The PCA uses a matrix indicating the degree of similarity between variables to calculate matrices that allow variables to be projected into a new space. Typically, the Pearson correlation coefficient is used as an index of similarity. When the latter is close to +1, these variables provide the same information. Table 3 shows the different correlations between the variables two by two.

Table 3. Groundwater correlation matrix in the Gadaïne-Ain Yaghout plain

*	Ca^{+2}	Mg^{+2}	Na^{+}	K^{+}	Cl^{-}	HCO_3^{-}	SO_4^{-}	NO_3^{-}	NO_2^{-}	PO_4^{-3}	NH_4^{+}	Fe^{2+}	Zn^{2+}	Cu^{2+}	Cd^{2+}	Sr^{2+}	O_2	CE	PH	T°
Ca^{+2}	1																			
Mg^{+2}	0.998	1																		
Na^{+}	0.864	0.867	1																	
K^{+}	0.496	0.504	0.426	1																
Cl^{-}	0.941	0.941	0.909	0.519	1															
HCO_3^{-}	1.000	0.998	0.864	0.496	0.941	1														
SO_4^{-}	0.615	0.622	0.653	0.253	0.576	0.615	1													
NO_3^{-}	-0.097	-0.090	0.144	-0.181	-0.003	-0.097	0.314	1												
NO_2^{-}	-0.006	-0.009	0.164	-0.091	0.004	-0.006	0.455	0.768	1											
PO_4^{-3}	0.165	0.180	0.217	0.333	0.217	0.165	0.496	0.604	0.469	1										
NH_4^{+}	0.575	0.575	0.674	0.260	0.630	0.575	0.743	0.616	0.621	0.688	1									
Fe^{2+}	0.039	0.046	0.265	-0.044	0.144	0.039	0.583	0.780	0.737	0.706	0.753	1								
Zn^{2+}	0.065	0.069	0.226	0.041	0.147	0.065	0.361	0.837	0.760	0.686	0.753	0.798	1							
Cu^{2+}	0.061	0.063	0.203	-0.102	0.141	0.061	0.517	0.576	0.480	0.576	0.651	0.857	0.654	1						
Cd^{2+}	0.852	0.851	0.876	0.532	0.896	0.852	0.418	-0.085	-0.112	0.106	0.511	0.013	0.045	0.009	1					
Sr^{2+}	0.941	0.943	0.936	0.520	0.954	0.941	0.689	0.084	0.128	0.296	0.715	0.257	0.236	0.264	0.872	1				
O_2	-0.122	-0.124	-0.226	-0.063	-0.234	-0.122	-0.388	-0.280	-0.250	-0.123	-0.278	-0.393	-0.329	-0.418	-0.028	-0.260	1			
CE	0.935	0.940	0.897	0.524	0.949	0.935	0.667	0.073	0.145	0.301	0.713	0.234	0.248	0.260	0.868	0.977	-0.257	1		
PH	-0.657	-0.654	-0.457	-0.297	-0.609	-0.657	-0.207	0.234	0.209	0.049	-0.266	0.161	-0.030	0.056	-0.609	-0.586	0.052	-0.625	1	
T°	-0.296	-0.292	-0.306	-0.009	-0.278	-0.297	-0.268	-0.180	-0.112	-0.302	-0.227	-0.201	-0.077	-0.189	-0.261	-0.306	0.031	-0.287	0.043	1

There is a strong bond between electrical conductivity and calcium, magnesium, sodium, chlorides, bicarbonates, and to a lesser degree with sulfates, which gives water of the chlorinated and sulfate calcium-magnesium type. These waters have acquired their chemical composition from the dissolution of evaporitic minerals such as halite (NaCl) and gypsum ($CaSO_4$, $2H_2O$). The presence of evaporites is confirmed by the high correlation between sodium and chloride ions (r = 0.9) and a good bond between calcium and sulfates (r = 0.61). A strong correlation between Ca^{2+} and Mg^{2+} is conditioned by the phenomenon of dolomitization. The good bond between Ca^{2+}, Mg^{2+}, Na^{+}, K^{+}, Cl^{-}, $SO4^{2-}$ and HCO^{3-} suggests that these elements may have a common origin. After the abuse of chemical fertilizers, good similarities appeared between nitrates and “phosphates”, between ammonium and “sulfates, nitrates”, thus between zinc and “nitrogenous elements, phosphates”, and finally between copper and “nitrogenous elements, phosphates, zinc”.

For this analysis, we will present only the projection of variables and individuals on the first factorial plane (F1-F2), which recovers the maximum of information contained in the entire table and has a total inertia of 73.2% (Table 4). The other dimensions provide little information, so it is not necessary to visualize them. To interpret the projection or the distribution of individuals on the factorial plane (F1-F2) (Fig. 8), it is necessary to make a correlation between the variables and factors F1 and F2 to construct a circular correlation graphs (Fig. 9).

Table 4. Inertia of the first two factorial axes

Factor	F1	F2
Own value	9.58	5.06
Variability (%)	47.89	25.33
% cumulative	47.89	73.21

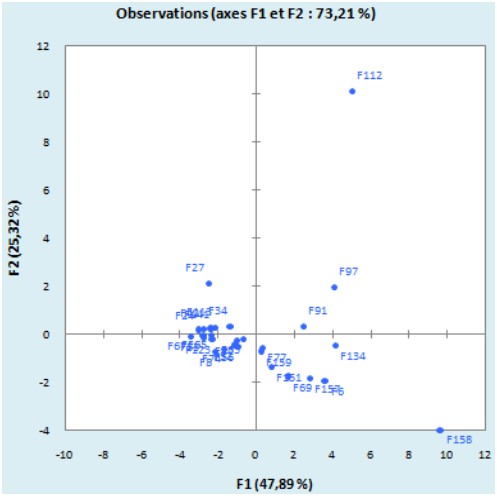

Figure 8. Distribution on the factorial plane (F1-F2)

The variables Ca^{2+}, Mg^{2+}, Na^{+}, K^{+}, Cl^{-}, SO_4^{2-}, HCO_3^{-}, NH_4^{+}, PO_4^{3-}, Cd^{2+}, Sr^{2+} EC and pH show a significant positive correlation, except for the pH, which shows a significant negative correlation with the first factor.

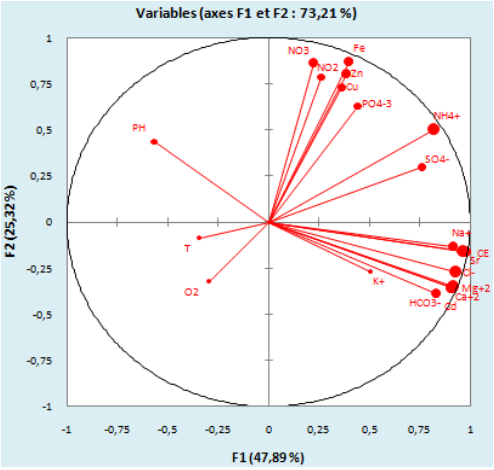

Figure 9. Circular correlation graphs of variables

While the elements NO_3^-, NO_2^-, PO_4^{3-}, Fe^{2+}, Zn^{2+} and Cu^{2+} indicate a significant positive correlation with F2 (Table 5).

Table 5. Correlations between variables and factors

Variable	F1	F2	Variable	F1	F2
Ca^{+2}	0.914	-0.355	NH_4^+	0.820	0.499
Mg^{+2}	0.916	-0.351	Fe^{+2}	0.398	0.869
Na^+	0.916	-0.131	Zn^{+2}	0.388	0.801
K^+	0.505	-0.271	Cu^{+2}	0.366	0.730
Cl^-	0.932	-0.272	Cd^{+2}	0.832	-0.389
HCO_3^-	0.914	-0.355	Sr^{+2}	0.975	-0.157
SO_4^-	0.761	0.295	O_2	-0.292	-0.326
NO_3^-	0.225	0.861	CE	0.968	-0.161
NO_2^-	0.263	0.785	pH	-0.562	0.436
PO_4^{-3}	0.440	0.628	T°	-0.344	-0.090

From Table 6, it is concluded that individuals F158 and F112 make the greatest contribution, compared with other observations, to the formation of the F1 and F2 successively. This is well represented by the graph in Figure 10.

Table 6. Contributions according to observations (%)

Individual	F1	F2	Individual	F1	F2
F6	5.017	2.626	F69	1.076	2.283
F8	1.707	0.358	F74	1.036	0.259
F16	2.755	0.000	F77	0.047	0.211
F24	3.409	0.018	F91	2.321	0.080
F27	2.322	3.162	F97	6.225	2.782
F34	0.641	0.075	F112	9.498	72.296
F42	2.843	0.042	F113	1.749	0.057
F47	0.379	0.040	F123	1.897	0.026
F52	0.406	0.159	F134	6.479	0.145
F53	2.838	0.011	F141	2.013	0.029
F56	0.342	0.189	F151	0.230	1.299
F63	0.158	0.027	F157	2.972	2.358
F65	2.080	0.000	F158	35.118	11.078
F67	4.419	0.004	F159	0.024	0.384

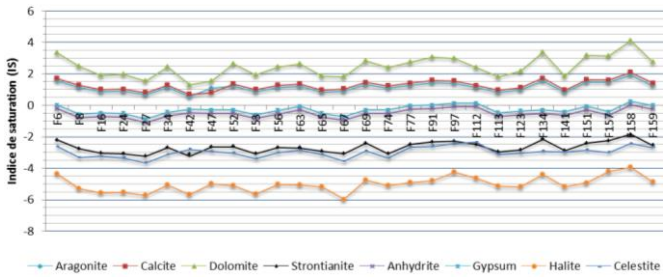

Figure 10. Variation of the saturation index for carbonate and evaporitic minerals

Similarly, for variables, we can note that the elements Ca^{2+}, Mg^{2+}, Na^+, Cl^-, SO_4^{2-}, SO_4^{2-}, HCO_3^-, NH_4^+, Cd^{2+} and CE make a great contribution to the construction of the first axis. On the other hand, NO_3^-, NO_2^-, PO_4^{3-}, Fe^{2+}, Zn^{2+} and Cu^{2+} participate to a large extent in the formation of the second factor, while pH also interacts along both axes (Table 7, Fig. 11).

Table 7. Contributions according to observations (%)

Variable	F1	F2	Variable	F1	F2
Ca^{+2}	8.716	2.493	PO_4^{-3}	2.022	7.794
Mg^{+2}	8.766	2.430	NH_4^+	7.022	4.919
Na^+	8.767	0.341	Fe^{+2}	1.653	14.916
K^+	2.668	1.449	Zn^{+2}	1.575	12.669
Cl^-	9.067	1.465	Cu^{+2}	1.396	10.528
HCO_3^-	8.717	2.492	Cd^{+2}	7.223	2.983
SO_4^-	6.040	1.717	Sr^{+2}	9.916	0.489
NO_3^-	0.528	14.633	CE	9.783	0.515
NO_2^-	0.720	12.169	pH	3.297	3.747
Ca^{+2}	8.716	2.493	PO_4^{-3}	2.022	7.794

	Carbonate minerals				Evaporite minerals			
	Aragonite	Calcite	Dolomite	Strontianite	Anhydrite	Gypsum	Halite	Celestite
	CaCO3	CaCO3	CaMg(CO3)2	$SrCO_3$	CaSO4	CaSO42H2O	NaCl	$SrSO_4$
Min	0,56	0,7	1,3	-3,22	-1,1	-0,88	-5,96	-3,65
Max	1,95	2,09	4,12	-1,85	0,03	0,25	-3,92	-2,35
Average	1,15	1,27	2,46	-2,66	-0,51	-0,29	-5,00	-2,98
SD	0,31	0,33	0,66	0,35	0,27	0,27	0,49	0,34

	Carbonate minerals				Evaporite minerals			
	Aragonite	Calcite	Dolomite	Strontianite	Anhydrite	Gypsum	Halite	Celestite
	CaCO3	CaCO3	CaMg(CO3)2	$SrCO_3$	CaSO4	CaSO42H2O	NaCl	$SrSO_4$
Min	0,56	0,7	1,3	-3,22	-1,1	-0,88	-5,96	-3,65
Max	1,95	2,09	4,12	-1,85	0,03	0,25	-3,92	-2,35
Average	1,15	1,27	2,46	-2,66	-0,51	-0,29	-5,00	-2,98
SD	0,31	0,33	0,66	0,35	0,27	0,27	0,49	0,34

Figure 11. Saturation index for mineral phases

In conclusion, the F1 factor maximizes inertia at 47% and represents highly mineralized water (CE) rich in Ca^{2+}, Mg^{2+}, Na^+, Cl^-, SO_4^{2-}, Sr^{2+} and HCO_3^-, thus polluted with NH_4^+ and Cd^{2+}. All these elements are inversely related to pH, which indicates its role in the dissolution of carbonate formations and silicates in contact with acidic waters. Therefore, F1 explains the predominant mechanisms for acquiring underground water mineralization in the Gadaïne-Ain Yaghout plain. Factor F2, which represents 25% of the information contained in the dataset, describes water polluted with NO_3^-, NO_2^-, PO_4^{3-}, Fe^{2+}, Cu^{2+} and Zn^{2+}.

A common source of these elements is the leaching of inorganic nitrogen fertilizers and manure. However, sewage effluents, as well as leaching from some geological formations, can create an additional origin for some of these elements. Thus, the second dimension can present water contaminated in general as a result of agricultural activities.

Regarding the study of individuals, the first main component is opposed to highly mineralized water points (F6, F69, F77, F9, F97, F112, F134, F151, F157, F158 and F159, of which sample F158 is the most loaded) among the weakly mineralized ones. Highly mineralized waters are not suitable for consumption and are located in chotts. While the second main component is opposed to the boreholes most polluted with NO_3^-, NO_2^-, PO_4^{3-}, Fe^{2+}, Cu^{2+} and Zn^{2+}, against the least affected by these elements, of which F112 water point is excessively polluted.

4.3.2. Calculation of saturation index for mineral phases

The study of the chemical equilibrium of groundwater and the states of their saturation in terms of mineral phases, first of all, requires the calculation of the ion activity. The calculated saturation index expresses the degree of chemical equilibrium between water and minerals in the aquifer matrix and can be viewed as a measure of the dissolution and/or precipitation process regarding the water-rock interaction. The saturation indices and chemical equilibria were calculated using the PHREEQC-2 software (version 2.10) (Fig. 11).

4.3.2.1. Saturation for carbonate minerals

The calculation of saturation indices covered only the most abundant carbonate minerals in sedimentary environments, namely calcite, aragonite ($CaCO_3$), dolomite ($CaMg(CO_3)_2$) and strontianite ($SrCO_3$). Calcite dissolution is a fast reaction and water can reach saturation by passing through the unsaturated zone. The samples show positive saturation index values (IS > 0) for calcite, aragonite and dolomite (Fig. 12a-d).

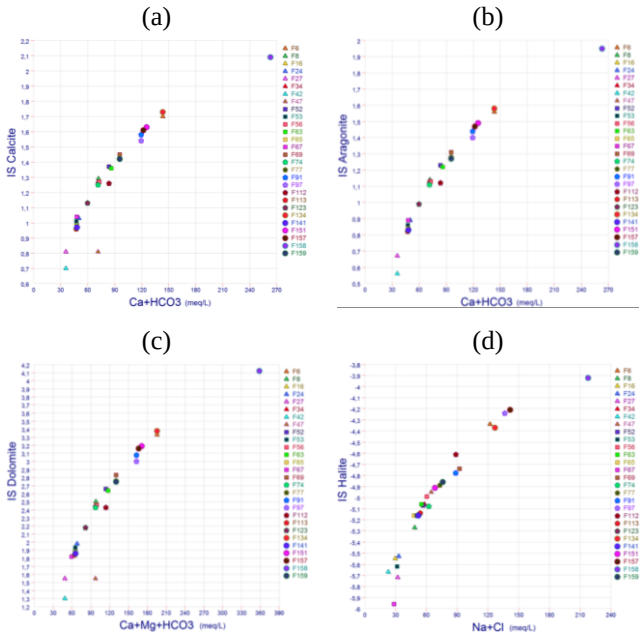

Figure 12. Saturation of groundwater: (a) for calcite as a function of Ca + HCO_3 concentration; (b) for aragonite as a function of Ca + HCO_3 concentration; (c) for dolomite as a function of Ca + Mg + HCO_3 concentration; (d) for halite as a function of Na + Cl concentration

In general, these indices range from 0.56 to 4.12, reflecting the state of precipitation of these minerals. On the other hand, strontianite has a negative saturation index that ranges from -1.85 to -3.22. These minerals arose as a result of the dissolution of limestone and dolomites from the Jurassic-Cretaceous period. This state of supersaturation indicates an excess of Ca^{+2} and Mg^{+2} ions, which inevitably results in very hard water.

Carbonate minerals vary in the same way and tend to precipitate mainly in the form of dolomite.

4.3.2.2. Saturation for evaporitic minerals

For evaporitic minerals, saturation indices for halite (NaCl), gypsum ($CaSO_4 \cdot 2H_2O$), anhydrite ($CaSO_4$) and celestite ($SrSO_4$) have been calculated. All samples from the studied aquifer system show negative saturation indices for halite (IS max = -3.92) and celestite (IS max = -2.35), testifying to the sub-saturation state of groundwater for these minerals. A large number of samples (78%) show a state of equilibrium with respect to gypsum, with the exception of six samples that are in the range of -0.51 < IS < -0.88. Therefore, they are undersaturated with this element. On the other hand, 10 samples are saturated with anhydrite (-0.47 < IS < 0.03), while most of the analyzed waters (64%) are undersaturated (-1.1 < IS < -0.47) for this element. Evaporitic minerals are predominantly in a state of undersaturation, even for Cl^-, SO_4^{-2} and Ca^{+2} ions, which have high concentrations in water. This is explained by the influence of high values of the equilibrium constant (log Ks) of evaporitic minerals $CaSO_4 \cdot 2H_2O$ (-4.58), $CaSO_4$ (-4.36), NaCl (1.58) and $SrSO_4$ (-6.63). On the other hand, for carbonate minerals, the equilibrium constant is lower ($CaMg(CO_3)_2$ (-17.09), $CaCO_3$ (-8.48) and $SrCO_3$ (-9.27), which leads to a higher saturation index and, hence, rapid precipitation of chemical elements (Fig. 13a-d).

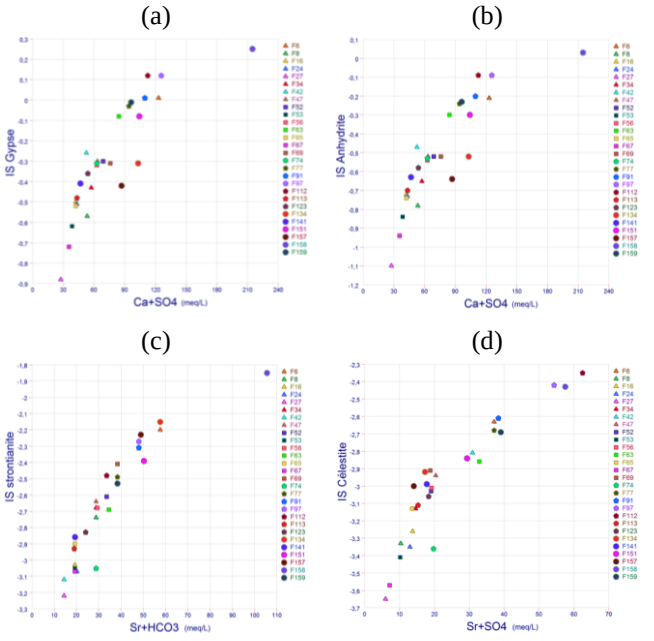

Figure 13. Saturation of groundwater: (a) for gypsum as a function of Ca + SO_4 concentration; (b) for strontianite as a function of Sr + HCO_3 concentration; (c) for celestite as a function of Sr + SO_4 concentration; (d) for anhydrite as a function of Ca + SO_4 concentration

Generally, the spatial distribution of saturation indices of carbonate and evaporitic minerals in both directions of groundwater circulation, the first of which is also the SE-NW direction, the second is from the overexploitation zone towards Tinsilt chott, where these indices reach their maximum values. In particular, the saturation indices of $CaSO_4 \cdot 2H_2O$ and $CaSO_4$ tend to balance at the level of the chotts. Here, the presence of gypsum, which seems to be one of the reasons for high SO_4^{-2} and Ca^{+2} contents, is subsequently confirmed by the positive correlation between Ca^{+2} and SO_4^{-2}. At the same time, magnesium is dissolved from the clays and marls present on the plain, as well as from the dolomites constituting the relief, which contributes to supersaturation with dolomite, calcite and aragonite and, consequently, their precipitation.

5. Conclusions

The hydro-geochemical behavior of the Gadaïne-Ain Yaghout aquifer waters has been studied using the hydrochemical and statistical tools. It has been revealed that rain-

water infiltration at the level of carbonate formations located on the boundaries of the studied area, where waters acquire their initial mineralization (carbonate) and are more mineralized in chlorides, sodium and sulfates upon contact with terrigenous saliferous formations of the Mio-Plio-Quaternary period. This determines the waters of calcium and magnesian chloride facies for all the waters of the plain.

The use of statistical tool makes it possible to show significant relationships between electrical conductivity and different chemical elements, thereby showing the strong participation of sulfates, chlorides and sodium in the acquisition of salinity. The enrichment in these elements coincides with the direction of groundwater flow (SE-NW), where these elements are highly concentrated in the center of the plain and at the level of the Tinsilt chott. The application of principal component analysis, as well as the calculation of the water saturation index has shown the existence of two water sources. One of them is a natural source, conditioned by the dissolution of carbonate and evaporite formations, and an entropic source, conditioned by the agricultural use of a vast plain in the study area with the abuse of nitrogen-containing products.

Acknowledgements

This work was conducted under the supervision of IAWRSMB-Tunisia and the Laboratory of Applied Research in Engineering Geology, Geotechnics, Water Sciences and the Environment, Setif 1 University, Algeria. We express our gratitude to the General Directorate of Scientific Research and Technological Development (DGRSDT-MESRS) for technical support. We are grateful to the editor and reviewers for their valuable improvement of the manuscript.

References

[1] Abdelhamid, K., & Abderrahmane, B. (2018). Study of the physical and chemical qualities of surface water and groundwater in the upper valley of wadi Rhumel (Eastern Algeria). *Arabian Journal of Geosciences*, *11*(5), 85. https://doi.org/10.1007/s12517-017-3380-7

[2] Saadali, B., Khedidja, A., Mihoubi, N., Ouddah, A., Djebassi, T., & Kouba, Y. (2020). Water quality assessment and organic pollution identification of Hammam-Grouz dam (Northeastern Algeria). *Arabian Journal of Geosciences*, *13*(20), 1-9. https://doi.org/10.1007/s12517-020-06117-9

[3] Hamed, Y., Hadji, R., Redhaounia, B., Zighmi, K., Bâali, F., & El Gayar, A. (2018). Climate impact on surface and groundwater in North Africa: A global synthesis of findings and recommendations. *Euro-Mediterranean Journal for Environmental Integration*, *3*(1), 25. https://doi.org/10.1007/s41207-018-0067-8

[4] Hamed, Y., Hadji, R., Ncibi, K., Hamad, A., Ben Sâad, A., Melki, A., & Mustafa, E. (2021). Modelling of potential groundwater artificial recharge in the transboundary Algero-Tunisian Basin (Tebessa-Gafsa): The application of stable isotopes and hydroinformatics tools. *Irrigation and Drainage*. https://doi.org/10.1002/ird.2647

[5] Ncibi, K., Hadji, R., Hajji, S., Besser, H., Hajlaoui, H., Hamad, A., & Hamed, Y. (2021). Spatial variation of groundwater vulnerability to nitrate pollution under excessive fertilization using index over-lay method in central Tunisia (Sidi Bouzid basin). *Irrigation and Drainage*, *70*(5), 1209-1226. https://doi.org/10.1002/ird.2599

[6] Rais, K., Kara, M., Gadri, L., Hadji, R., & Khochmen, L. (2017). Original approach for the drilling process optimization in open cast mines; case study of Kef Essenoun open pit mine Northeast of Algeria. *Mining Science*, (24), 147-159. https://doi.org/10.5277/msc172409

[7] Zahri, F., Boukelloul, M.L., Hadji, R., & Talhi, K. (2016 Slope stability analysis in open pit mines of Jebel Gustar career, NE Algeria – A multi-steps approach. *Mining Science*, (23), 137-146. https://doi.org/10.5277/msc162311

[8] Khedidja, A., & Boudoukha, A. (2019). Quality assessment of shallow groundwater for irrigation purposes in Tadjenanet – Chelghoum Laid area (Eastern Algeria). *International Journal of River Basin Management*, *19*(2), 141-148. https://doi.org/10.1080/15715124.2019.1628031

[9] Hamad, A., Abdeslam, I., Fehdi, C., Badreddine, S., Mokadem, N., Legrioui, R., Hadji, R., & Hamed, Y. (2021). Vulnerability characterization for multi-carbonate aquifer systems in semiarid climate, case of Algerian-Tunisian transboundary basin. *International Journal of Energy and Water Resources*, 1-14. https://doi.org/10.1007/s42108-021-00142-4

[10] Hamad, A., Hadji, R., Boubaya, D., Brahmi, S., Baali, F., Legrioui, R., & Hamed, Y. (2021). Integrating gravity data for structural investigation of the Youkous-Tebessa and Foussana-Talah trans-boundary basins (North Africa). *Euro-Mediterranean Journal for Environmental Integration*, *6*(2), 1-11. https://doi.org/10.1007/s41207-021-00270-7

[11] Benmarce, K., Hadji, R., Zahri, F., Khanchoul, K., Chouabi, A., Zighmi, K., & Hamed, Y. (2021). Hadrochemical and geothermometry characterization for a geothermal system in semiarid dry climate: The case study of Hamma spring (northeast Algeria). *Journal of African Earth Sciences*, 104285. https://doi.org/10.1016/j.jafrearsci.2021.104285

[12] Nekkoub, A., Baali, F., Hadji, R., & Hamed, Y. (2020). The EPIK multi-attribute method for intrinsic vulnerability assessment of karstic aquifer under semi-arid climatic conditions, case of Cheria Plateau, NE Algeria. *Arabian Journal of Geosciences*, *13*(15), 1-15. https://doi.org/10.1007/s12517-020-05704-0

[13] Khedidja, A., & Boudoukha, A. (2014). Risk assessment of agricultural pollution on groundwater quality in the high valley of Tadjenanet-Chelghoum Laid (Eastern Algeria). *Desalination and Water Treatment*, *52*(22-24), 4174-4182. https://doi.org/10.1080/19443994.2013.874702

[14] Khedidja, A., & Boudoukha, A. (2016). Statistical and hydro-chemical characterization of the shallow aquifer of Tadjnanet-Chelghoum laid (Eastern Algeria). *LARHYSS Journal*, (28), 181-197.

[15] Mokadem, N., Demdoum, A., Hamed, Y., Bouri, S., Hadji, R., Boyce, A., Laouar, R., & Saad, A. (2016). Hydrogeochemical and stable isotope data of groundwater of a multi-aquifer system: Northern Gafsa basin e Central Tunisia. *Journal of African Earth Sciences*, (114), 174-191. https://doi.org/10.1016/j.jafrearsci.2015.11.010

[16] Ncibi, K., Hadji, R., Hamdi, M., & Mokadem, N. (2020). Application of the analytic hierarchy process to weight the criteria used to determine the Water Quality Index of groundwater in the northeastern basin of the Sidi Bouzid region, Central Tunisia. *Euro-Mediterranean Journal for Environmental Integration*, (5), 1-15. https://doi.org/10.1007/s41207-020-00159-x

[17] Ncibi, K., Chaar, H., Hadji, R., Baccari, N., Sebei, A., Khelifi, F., & Hamed, Y. (2020). A GIS-based statistical model for assessing groundwater susceptibility index in shallow aquifer in Central Tunisia (Sidi Bouzid basin). *Arabian Journal of Geosciences*, *13*(2), 98. https://doi.org/10.1007/s12517-020-5112-7

[18] Brahmi, S., Baali, F., Hadji, R., Brahmi, S., Hamad, A., Rahal, O., & Hamed, Y. (2021). Assessment of groundwater and soil pollution by leachate using electrical resistivity and induced polarization imaging survey, case of Tebessa municipal landfill, NE Algeria. *Arabian Journal of Geosciences*, *14*(4), 1-13. https://doi.org/10.1007/s12517-021-06571-z

[19] Besser, H., Mokadem, N., Redhaounia, B., Hadji, R., & Hamed, Y. (2018). Groundwater mixing and geochemical assessment of low-enthalpy resources in the geothermal field of southwestern Tunisia. *Euro-Mediterranean Journal for Environmental Integration*, *3*(1), 16. https://doi.org/10.1007/s41207-018-0055-z

[20] Besser, H., Dhaouadi, L., Hadji, R., & Hamed, Y. (2021). Ecologic and economic perspectives for sustainable irrigated agriculture under arid climate conditions: An analysis based on environmental indicators for southern Tunisia. *Journal of African Earth Sciences*, 104-134. https://doi.org/10.1016/j.jafrearsci.2021.104134

[21] Savci, S. (2012). An agricultural pollutant: chemical fertilizer. *International Journal of Environmental Science and Development*, *3*(1), 73. https://doi.org/10.7763/IJESD.2012.V3.191

[22] Hamed, Y., Ahmadi, R., Hadji, R., Mokadem, N., Ben Dhia, H., Ali, W. (2014). Groundwater evolution of the Continental Intercalaire aquifer of Southern Tunisia and a part of Southern Algeria: Use of geochemical and isotopic indicators. *Desalination and Water Treatment*, *52*(10-12), 1990-1996. https://doi.org/10.1080/19443994.2013.806221

[23] Hamed, Y., Redhaounia, B., Ben Sâad, A., Hadji, R., & Zahri, F. (2017). Groundwater inrush caused by the fault reactivation and the climate impact in the mining Gafsa basin (southwestern Tunisia). *Journal of Tethys*, *5*(2), 154-164.

[24] Hamed, Y., Redhaounia, B., Sâad, A., Hadji, R., Zahri, F., & Zighmi, K. (2017). Hydrothermal waters from karst aquifer: Case study of the Trozza basin (Central Tunisia). *Journal of Tethys*, *5*(1), 33-44.

[25] Batayneh, A., Ghrefat, H., Zaman, H., Mogren, S., Zumlot, T., Elawadi, E. (2012). Assessment of the physicochemical parameters and heavy metals toxicity: application to groundwater quality in unconsolidated shallow aquifer system. *Research Journal of Environmental Toxicology*, *6*(5), 169. https://doi.org/10.3923/rjet.2012.169.183

[26] Batsaikhan, B., Yun, S.T., Kim, K.H., Yu, S., Lee, K.J., & Lee, Y.J. (2021). Groundwater contamination assessment in Ulaanbaatar City, Mongolia with combined use of hydrochemical, environmental isotopic, and statistical approaches. *Science of the Total Environment*, (765), 142790. https://doi.org/10.1016/j.scitotenv.2020.142790

[27] Hamad, A., Hadji, R., Bâali, F., Houda, B., Redhaounia, B., Zighmi, K., & Hamed, Y. (2018). Conceptual model for karstic aquifers by combined analysis of GIS, chemical, thermal, and iso-topic tools in Tuniso-Algerian transboundary basin. *Arabian Journal of Geosciences*, *11*(15), 409. https://doi.org/10.1007/s12517-018-3773-2

[28] Hamad, A., Baali, F., Hadji, R., Zerrouki, H., Besser, H., Mokadem, N., & Hamed, Y. (2018). Hydrogeochemical characterization of water mineralization in Tebessa-Kasserine karst system (Tuniso-Algerian Transboundry basin). *Euro-Mediterranean Journal for Environmental Integration*, *3*(1), 7. https://doi.org/10.1007/s41207-017-0045-6

[29] Thuyet, D.Q., Saito, H., Saito, T., Moritani, S., Kohgo, Y., & Komatsu, T. (2016). Multivariate analysis of trace elements in shallow groundwater in Fuchu in western Tokyo Metropolis, Japan. *Environmental Earth Sciences*, *75*(7), 1-14. https://doi.org/10.1007/s12665-015-5170-4

[30] Zhang, H., Bian, J., & Wan, H. (2021). Hydrochemical appraisal of groundwater quality and pollution source analysis of oil field area: A case study in Daqing City, China. *Environmental Science and Pollution Research*, *28*(15), 18667-18685. https://doi.org/10.1007/s11356-020-12059-2

[31] Athamena, A., & Menani, M.R. (2018). Nitrogen flux and hydrochemical characteristics of the calcareous aquifer of the Zana plain, north east of Algeria. *Arabian Journal of Geosciences*, *11*(13), 1-14. https://doi.org/10.1007/s12517-018-3681-5

[32] Tamani, F., Hadji, R., Hamad, A., & Hamed, Y. (2019) Integrating remotely sensed and GIS data for the detailed geological mapping in semi-arid regions: Case of Youks les Bains Area, Tebessa Province, NE Algeria. *Geotechnical and Geological Engineering*, 1-11.

[33] Demdoum, A., Hamed, Y., Feki, M., & Hadji, R. (2015). Multi-tracer investigation of groundwater in El Eulma Basin (NW Algeria), North Africa. *Arabian Journal of Geosciences*, *8*(5), 3321-3333.

[34] Argamasilla, M., Barberá, J.A., & Andreo, B. (2017). Factors controlling groundwater salinization and hydrogeochemical processes in coastal aquifers from southern Spain. *Science of the Total Environment*, (580), 50-68. https://doi.org/10.1016/j.scitotenv.2016.11.173

[35] Abbasi, T., & Abbasi, S.A. (2011). Sources of pollution in rooftop rainwater harvesting systems and their control. *Critical Reviews in Environmental Science and Technology*, *41*(23), 2097-2167. https://doi.org/10.1080/10643389.2010.497438

[36] Rouabhia, A., Djabri, L., Hadji, R., Baali, F., Fahdi, Ch., & Hanni, A. (2012). Geochemical characterization of groundwater from shallow aquifer surrounding Fetzara Lake NE Algeria. *Arabian Journal of Geosciences*, *5*(1), 1-13. https://doi.org/10.1007/s12517-010-0202-6

[37] Mouici, R, Baali, F, Hadji, R, Boubaya, D, Audra, P., Fehdi, C.É., & Arfib, B. (2017). Geophysical, geotechnical, and speleologic assessment for karst-sinkhole collapse genesis in Cheria plateau (NE Algeria). *Mining Science*, (24), 59-71. https://doi.org/10.5277/msc172403

[38] Zghibi, A., Merzougui, A., Zouhri, L., & Tarhouni, J. (2014). Understanding groundwater chemistry using multivariate statistics techniques to the study of contamination in the Korba unconfined aquifer system of Cap-Bon (North-east of Tunisia). *Journal of African Earth Sciences*, (89), 1-15. https://doi.org/10.1016/j.jafrearsci.2013.09.004

[39] Matta, G., Srivastava, S., Pandey, R.R., & Saini, K.K. (2017). Assessment of physicochemical characteristics of Ganga Canal water quality in Uttarakhand. *Environment, Development and Sustainability*, *19*(2), 419-431. https://doi.org/10.1007/s10668-015-9735-x

[40] Appelo, C.A.J., & Postma, D. (2004). *Geochemistry, groundwater and pollution*. London, United Kingdom: CRC press, 683 p. https://doi.org/10.1201/9781439833544

[41] Rodier, J., Bazin, C., Broutin, J.C., Chambon, P., Champsaur, H., & Rodi, L. (1996). *L 'analyse de l 'eau*. Paris, France: Dunod, 1383 p.

[42] Manchar, N., Benabbas, C., Hadji, R., Bouaicha, F., & Grecu, F. (2018). Landslide susceptibility assessment in Constantine region (NE Algeria) by means of statistical models. *Studia Geotechnica et Mchanica*, *40*(3), 208-219. https://doi.org/10.2478/sgem-2018-0024

[43] Dahoua, L., Yakovitch, S.V., & Hadji, R.H. (2017). GIS-based technic for roadside-slope stability assessment: An bivariate approach for A1 East-west highway, North Algeria. *Mining Science*, (24), 117-127. https://doi.org/10.5277/msc172407

[44] Hadji, R., Limani, Y., & Demdoum, A. (2014). Using multivariate approach and GIS applications to predict slope instability hazard case study of Machrouha municipality, NE Algeria. In *1st International Conference on Information and Communication Technologies for Disaster Management* (pp. 1-10). https://doi.org/10.1109/ICT-DM.2014.6917787

[45] El Mekki, A., Hadji, R., & Chemseddine, F. (2017). Use of slope failures inventory and climatic data for landslide susceptibility, vulnerability, and risk mapping in souk Ahras region. *Mining Science*, (24), 237-245. https://doi.org/10.5277/msc172417

[46] Anis, Z., Wissem, G., Riheb, H., Biswajeet, P., & Essghaier, G.M. (2019). Effects of clay properties in the landslides genesis in flysch massif: Case study of Aïn Draham, North Western Tunisia. *Journal of African Earth Sciences*, (151), 146-152. https://doi.org/10.1016/j.jafrearsci.2018.12.005

[47] Valocchi, A.J. (2012). Hydrogeochemical models. In *Delivery and Mixing in the Subsurface* (pp. 77-116). https://doi.org/10.1007/978-1-4614-2239-6_4

[48] Parkhurst, D.L., & Appelo, C.A.J. (2013). *Description of input and examples for PHREEQC version 3-a computer program for speciation, batch-reaction, one-dimensional transport, and inverse geochemical calculations*. Chapter 43 of Section A, Groundwater Book 6, Modeling Techniques. Colorado, United States: US Geological Survey, 519 p.

[49] Bencer, S., Boudoukha, A., & Mouni, L. (2016). Multivariate statis-tical analysis of the groundwater of Ain Djacer area (Eastern of Algeria). *Arabian Journal of Geosciences*, (9), 248. https://doi.org/10.1007/s12517-015-2277-6

[50] Bensoltane, M.A., Zeghadnia, L., & Hadji, R. (2021). Physicochemical characterization of drinking water quality of the communal water distribution network in Souk Ahras City/Algeria. *Civil Engineering Research Journal*, *12*(02), 1-6. https://doi.org/10.19080/CERJ.2021.12.555834

Багатоваріантний статистичний підхід до фізико-хімічного характеру зміни мілководних ґрунтових вод у напівпосушливому сухому кліматі: дослідження на прикладі рівнини Гадаїн-Айн Ягхут у північно-східному Алжирі

І. Діб, А. Хедіджа, В. Чаттах, Р. Хаджі

Мета. Встановлення механізмів набуття мінералізації в замкнутих водоносних горизонтах під впливом природних та антропогенних факторів на основі застосування багатоваріантних статистичних методів.

Методика. Прийнятий метод вимірює хімічне виділення Ca^{+2}, Mg^{+2}, Na^{+}, K^{+}, HCO^{-3}, Cl^{-}, SO_4^{-2}, NO^{-3}, NO^{-2}, NH^{+4} і PO_4^{-3} за допомогою атомно-абсорбційного спектрометру. Вміст азоту та розчиненого кисню вимірюють за допомогою спектрофотометра. Температура (T°), електропровідність (EC), pH і розчинений кисень визначаються за допомогою багатопараметричної системи.

Результати. Встановлено, що 28 проб води з міо-пліо-четвертичного водоносного горизонту рівнини Гадаїн-Айн Ягхут мають хімічні фації хлоридного, сульфатно-кальцієвого та хлоридно-магнієвого типів. Результати показують значну варіацію в концентраціях хімічних елементів, які в деяких випадках перевищують стандарти придатності для пиття. Мінералізація в основному спричинена розчиненням мінералів, що випаровуються, саме таких як гіпс, галіт і епсоміт.

Наукова новизна. Доведено, що вода набуває карбонатної мінералізації на межі водопостачання, тоді як хлоридну, натрієву та сульфатну мінералізацію вона набуває при контакті з теригенними соленосними утвореннями, а також у взаємодії з соляними чотовими утвореннями. Це визначає води хлоридно-кальцієвих та хлоридно-магнезіальних фацій для всіх вод рівнини.

Практична значимість. Практичне цінність цього дослідження полягає у зручності багатовимірної статистичної оцінки складних фізико-хімічних баз даних у визначенні джерел забруднення та розумінні часових коливань для ефективного управління якістю підземних вод у напівпосушливих регіонах.

Ключові слова: *напівпосушливий, неглибокий водоносний горизонт, фізико-хімічний, багатоваріантний, забруднення*